Quantum color image scaling based on bilinear interpolation

Chao Gao(高超)[1,2], Ri-Gui Zhou(周日贵)[1,2,†], and Xin Li(李鑫)[1,2]

[1] *College of Information Engineering, Shanghai Maritime University, Shanghai* 201306, *China*
[2] *Research Center of Intelligent Information Processing and Quantum Intelligent Computing, Shanghai* 201306, *China*

(Received 12 May 2022; revised manuscript received 14 August 2022; accepted manuscript online 5 September 2022)

As a part of quantum image processing, quantum image scaling is a significant technology for the development of quantum computation. At present, most of the quantum image scaling schemes are based on grayscale images, with relatively little processing for color images. This paper proposes a quantum color image scaling scheme based on bilinear interpolation, which realizes the $2^{n_1} \times 2^{n_2}$ quantum color image scaling. Firstly, the improved novel quantum representation of color digital images (INCQI) is employed to represent a $2^{n_1} \times 2^{n_2}$ quantum color image, and the bilinear interpolation method for calculating pixel values of the interpolated image is presented. Then the quantum color image scaling-up and scaling-down circuits are designed by utilizing a series of quantum modules, and the complexity of the circuits is analyzed. Finally, the experimental simulation results of MATLAB based on the classical computer are given. The ultimate results demonstrate that the complexities of the scaling-up and scaling-down schemes are quadratic and linear, respectively, which are much lower than the cubic function and exponential function of other bilinear interpolation schemes.

Keywords: quantum image processing, image scaling, quantum image representation, bilinear interpolation

PACS: 03.67.–a, 03.67.Ac, 03.67.Lx, 07.05.Pj **DOI:** 10.1088/1674-1056/ac8f35

1. Introduction

Compared with the classical computing, quantum computation is a novel field, but many researchers have been engaged in extensive research. In 1982, Feynman proposed a novel computer model,[1] named quantum computer. With its powerful parallel processing capabilities, quantum computer far exceeds the computational processing speed of classical computer. The quantum Turing machine was proposed for the first time in 1985.[2] Since then, many quantum algorithms were proposed successively, such as a large integer decomposition algorithm proposed by Shor[3] and database search algorithm proposed by Grover.[4] The proposals of these quantum algorithms have demonstrated the feasibility of the powerful parallel processing capability of quantum computation.

Quantum image processing (QImP) is a vital branch of quantum computation. As an emerging interdisciplinary subject, QImP currently has two mainstream research directions, namely, quantum image representation and quantum image processing algorithm.

The objective of quantum image representation (QIR) is to store the classical digital images in quantum computer in the form of qubits by utilizing quantum image representation model. In 2003, Venegas-Andraca *et al.*[5] proposed the first quantum image representation model, named qubit lattice model, using the method of holding one pixel by one qubit. In 2005, Latorre[6] proposed the real ket model utilizing quantum superposition to store image information. After that, Venegas-Andraca[7] introduced a novel model again, named entangled image, which can represent an image by storing geometrical shapes in quantum system. Since then, many widely used quantum image representation models have been proposed, such as FRQI,[8] NEQR,[9] NAQSS,[10] and NCQI.[11] The NCQI representation model has become one of the most commonly accepted QIRs nowadays because of its pinpoint accuracy.

As another critical branch of QIP, quantum image processing algorithm is also a popular research field at present, including the simple geometric transformation,[12] color transformation,[13] feature extraction,[14] image translation,[15] image scaling,[16–19] image scrambling,[20,21] image segmentation[22] and image encryption.[23,24] For the quantum image scaling, the main purpose is to resize a digital image. Similar to but somewhat different from quantum geometric transformation, quantum image scaling utilizes the virous interpolation methods to generate new pixels or delete redundant pixels, so as to enlarge or reduce the digital images. At present, interpolation methods commonly employed in classical image scaling schemes include nearest-neighbor, bilinear and bicubic interpolation.[25] However, until now, the first two interpolation methods mentioned above are still utilized in quantum grayscale image scaling, while only the nearest-neighbor interpolation method is employed in quantum color image scaling.

In this paper, a quantum color image scaling scheme based on bilinear interpolation is proposed for the first time. Inspired by NCQI, the improved NCQI (INCQI)[26] is de-

†Corresponding author. E-mail: rgzhou@shmtu.edu.cn

© 2023 Chinese Physical Society and IOP Publishing Ltd

scribed to scale the $2^{n_1} \times 2^{n_2}$ quantum color image to $2^{m_1} \times 2^{m_2}$. In this scheme, the complexities of the scaling-up circuit and the scaling-down circuit are quadratic function and linear function respectively, while the complexity of other quantum image scaling schemes so far are almost always a cubic function or even an exponential function. Furthermore, the experimental results demonstrate that the proposed scheme has the superior scaling effect than another scheme in Ref. [19].

The rest of this paper is organized as follows. The theoretical basis including the INCQI representation model and bilinear interpolation method is introduced in Section 2. In Section 3, a series of quantum modules utilized in the quantum color image scaling circuits are briefly described. In Section 4, the interrelated procedures, quantum circuits to realize quantum color image scaling are given, and the complexity of the related circuits is analyzed. Section 5 shows the result of the simulation experiment and makes a comparison with another scheme based on nearest-neighbor interpolation. Finally, the conclusion and future works are given in Section 6.

2. Theoretical basis

2.1. A novel quantum representation of color digital images (NCQI)

In 2016, Sang *et al.*[11] proposed a novel quantum representation of color digital image, i.e., NCQI. For a $2^n \times 2^n$ color digital image, its representation of NCQI is described as follows:

$$|I\rangle = \frac{1}{2^n} \sum_{Y=0}^{2^n-1} \sum_{X=0}^{2^n-1} |C(Y,X)\rangle \otimes |YX\rangle, \tag{1}$$

where $|Y\rangle$ and $|X\rangle$ denote the vertical position and horizontal position, respectively. $|C(Y,X)\rangle$ denotes the value information of the corresponding pixel, which can be encoded by the binary sequence as below:

$$\begin{aligned} |C(Y,X)\rangle &= |R(Y,X)\,G(Y,X)\,B(Y,X)\rangle \\ &= \left|\underbrace{R_{q-1}\ldots R_0}_{\text{Red}}\ \underbrace{G_{q-1}\ldots G_0}_{\text{Green}}\ \underbrace{B_{q-1}\ldots B_0}_{\text{Blue}}\right\rangle. \end{aligned} \tag{2}$$

The value range of every channel (RGB) is $[0,\ 2^q-1]$. Equation (1) indicates that the whole NCQI model is stored into a normalized quantum superposition state. For one pixel of a quantum color image with three channels (R,G,B), NCQI model consists of three portions: $|C(Y,X)\rangle$ representing color information, $|Y\rangle$ representing the vertical position information, and $|X\rangle$ representing the horizontal position information. According to Eq. (1), $2n+3q$ qubits are employed to store a $2^n \times 2^n$ quantum color digital image with every channel (R,G,B) ranged $[0,2^q-1]$ into NCQI state.

2.2. The improved NCQI

With regard to the quantum image scaling, when the scaling ratios of the two dimensions are diverse, the NCQI model that can only represent an image of size $2^n \times 2^n$ cannot be applied. In order to solve the problem, Zhou *et al.*[26] the improved NCQI (INCQI) is proposed to represent quantum images having $2^{n_1} \times 2^{n_2}$ pixels as described below:

$$|I\rangle = \frac{1}{2^{\frac{n_1+n_2}{2}}} \sum_{Y=0}^{2^{n_1}-1} \sum_{X=0}^{2^{n_2}-1} |C(Y,X)\rangle\,|YX\rangle, \tag{3}$$

where

$$\begin{aligned} |YX\rangle &= |Y\rangle\,|X\rangle \\ &= |y_0 y_1 \ldots y_{n_1-1}\rangle\,|x_0 x_1 \ldots x_{n_2-1}\rangle,\ \ y_i, x_i \in \{0,1\}, \\ |C(Y,X)\rangle &= |R(Y,X)\,G(Y,X)\,B(Y,X)\,, \\ &= \left|\underbrace{R_{q-1}\ldots R_0}_{\text{Red}}\ \underbrace{G_{q-1}\ldots G_0}_{\text{Green}}\ \underbrace{B_{q-1}\ldots B_0}_{\text{Blue}}\right\rangle. \end{aligned} \tag{4}$$

INCQI utilizes $Y(n_1$ qubits), $X(n_2$ qubits) and $C(Y,X)$ ($3q$ qubits) to represent the Y-coordinate, X-coordinate and pixel values of a quantum color image,[26] respectively. A simple example of a 4×2 INCQI color image and its corresponding representation are given in Fig. 1.

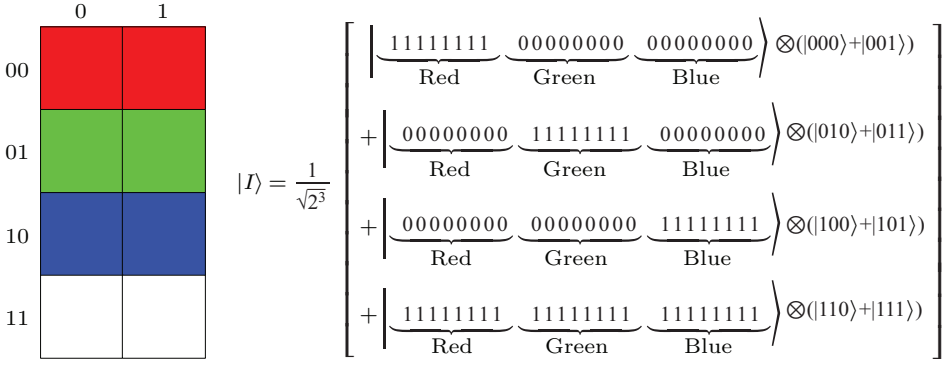


Fig. 1. An example of a 4×2 color image and its INCQI expression.

2.3. Bilinear interpolation method

In the classical image scaling, no matter the scheme of scaling-up or scaling-down, the interpolation methods will inevitably be employed. The purpose of interpolation method is to modify a digital image by generating new pixels or deleting redundant pixels. There are three commonly used interpolation methods: nearest-neighbor, bilinear and bicubic. Among them, the image scaling effect of bicubic interpolation is optimal, followed by the bilinear interpolation, and the nearest-neighbor interpolation is relatively unsatisfactory. However, as the improvement of scaling effect, the corresponding computational complexity will also increase.

In this paper, bilinear interpolation is opted as the interpolation method of the color image scaling. However, in this proposed scaling-down scheme, the pixel value of the interpolated image is determined by one pixel value of the corresponding original image. Consequently, the scaling-down scheme in this paper is based on the not rigorous bilinear interpolation. The concrete quantum color image scaling scheme will be elaborated explicitly in Section 4.

The bilinear interpolation method usually employed in two dimensions of images, vertical and horizontal, and its corresponding function expression is described as follows:

$$\begin{aligned} I' &= S(I, r_x, r_y) = S_y(S_x(I, r_x), r_y) \\ &= S_x(S_y(I, r_y), r_x), \end{aligned} \tag{5}$$

where I corresponds to the original image, I' represents the scaled image, S is the scaling function, and r_y and r_x are the vertical and horizontal scaling ratios, respectively. The function S can be decomposed into S_y and S_x, which are the vertical and horizontal scaling functions, respectively. The principle of S_y and S_x are exactly the same and can be interchanged. Therefore, regardless of which dimension is scaled firstly, the final scaled image is exactly the same.

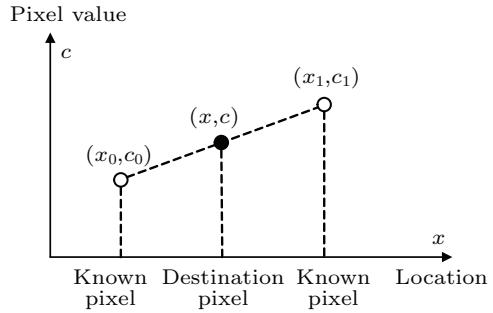


Fig. 2. The bilinear interpolation in X direction.

The bilinear interpolation method in X direction is described in Fig. 2, where the destination pixel (x,c) can be calculated from the pixels (x_0,c_0) and (x_1,c_1). The concrete linear relationship is given as follows:

$$\frac{c-c_0}{x-x_0} = \frac{c_1-c}{x_1-x}. \tag{6}$$

Consequently, the pixel value c can continue to be converted into

$$c = \frac{(x_1-x)c_0 + (x-x_0)c_1}{x_1-x_0}. \tag{7}$$

Assume that a $2^{n_1} \times 2^{n_2}$ original image is scaled to the interpolated image of size $2^{m_1} \times 2^{m_2}$. Then the color value $f(Y',X')$ of position (Y',X') in the interpolated image can be calculated by the bilinear interpolation function of the four adjacent pixels (Y,X), $(Y+1,X)$, $(Y,X+1)$ and $(Y+1,X+1)$ in the original image. The mapping relationship of these pixels is given in Fig. 3. Here,

$$\begin{aligned} &Y = \left\lfloor Y' \times \frac{2^{n_1}}{2^{m_1}} \right\rfloor, \quad X = \left\lfloor X' \times \frac{2^{n_2}}{2^{m_2}} \right\rfloor, \\ &d_y = \frac{2^{n_1}}{2^{m_1}} Y' - Y, \quad d_x = \frac{2^{n_2}}{2^{m_2}} X' - X. \end{aligned} \tag{8}$$

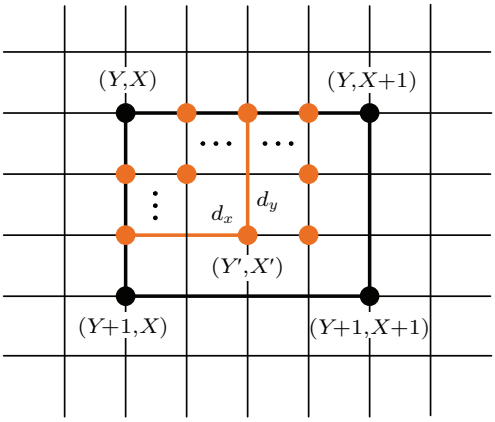


Fig. 3. Mapping relationship of coordinates in two images.

Based on the above coordinate mapping relationship, the color value $f(Y',X')$ of the position (Y',X') in the interpolation image can be calculated as follows:

$$\begin{aligned} &\begin{cases} f(Y',X')_a = (1-d_x) f(Y,X) + d_x f(Y,X+1) \\ f(Y',X')_b = (1-d_x) f(Y+1,X) + d_x f(Y+1,X+1) \end{cases} \\ \Rightarrow\ & f(Y',X') = (1-d_y) f(Y',X')_a + d_y f(Y',X')_b \\ =\ & (1-d_x)(1-d_y) f(Y,X) + d_x (1-d_y) f(Y,X+1) \\ & + (1-d_x) d_y f(Y+1,X) + d_x d_y f(Y+1,X+1). \end{aligned} \tag{9}$$

3. Quantum modules

In this section, a series of quantum modules utilized in the proposed quantum color image scaling circuits will be briefly introduced, including multiple CNOT module, U_1 module, $\Omega_{Y,X}$ module, adder module, RS module, TM module and divided by 2 module. Meanwhile, the functions of these quantum modules and their corresponding quantum circuits will be expounded.

3.1. Multiple CNOT module

The function of multiple CNOT module is to copy qubits,[27] and its quantum circuit is shown in Fig. 4. In order to replicate $|Y\rangle = |Y_{n-1}\ldots Y_1 Y_0\rangle$, n ancillary qubits and n CNOT-gates are employed to complete this function. In this quantum circuit, the qubits $|Y\rangle \otimes |0\rangle^{\otimes n}$ as the input part are converted into the output $|Y\rangle \otimes |Y\rangle$.

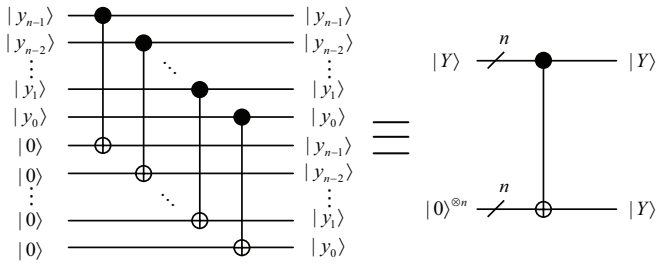


Fig. 4. The quantum circuit of multiple CNOT module.

3.2. Adding one module U_1

The function of adding one module U_1 is to execute the plus one operation if and only if $x_{n-1}\times\cdots\times x_1\times x_0 \neq 1$, i.e.,

$$U_1|x_{n-1}\ldots x_1 x_0\rangle = \begin{cases} |x_{n-1}\ldots x_1 x_0+1\rangle, & x_{n-1}\times\cdots\times x_1\times x_0\neq 1, \\ |x_{n-1}\ldots x_1 x_0\rangle, & x_{n-1}\times\cdots\times x_1\times x_0 = 1, \end{cases} \tag{10}$$

where n is a positive integer, $n\geq 1$, and $x_0, x_1, \ldots, x_{n-1} \in \{0,1\}$

Figure 5 describes a detailed quantum circuit of the U_1 module.

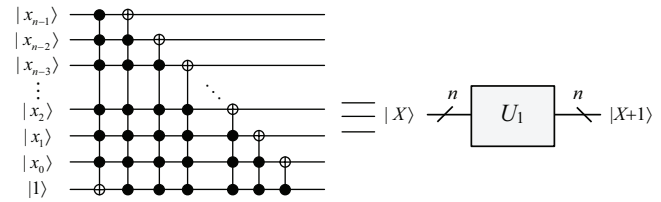


Fig. 5. The quantum circuit of U_1 module.

3.3. Quantum operation $\Omega_{Y,X}$

The function of unitary operation $\Omega_{Y,X}$[9] is to set the pixel value of position (Y,X) in the quantum image, and its expression is as follows:

$$\Omega_{Y,X} = \bigotimes_{i=0}^{3q-1} \Omega^i_{Y,X}, \quad \Omega^i_{Y,X}: |0\rangle \to |0\oplus C^i_{Y,X}\rangle, \tag{11}$$

where $3q$ qubits and $|C_{Y,X}\rangle$ represent the color depth of the quantum color image and the color value of the position (Y,X), respectively.

Based on the INCQI model, $\Omega_{Y,X}$ is a (n_1+n_2)-CNOT gate when $C^i_{Y,X}=1$. Otherwise, it is a quantum identity gate that does not change the initial state $|0\rangle$. Consequently, for a quantum color image with the color depth $3q$, the realization process of quantum operation $\Omega_{Y,X}$ is described below:

$$\begin{aligned}\Omega_{Y,X}|0\rangle^{\otimes 3q} &= \bigotimes_{i=0}^{3q-1}(\Omega^i_{Y,X}|0\rangle) = \bigotimes_{i=0}^{3q-1}|0\oplus C^i_{Y,X}\rangle \\ &= \bigotimes_{i=0}^{3q-1}|C^i_{Y,X}\rangle = |C(Y,X)\rangle. \end{aligned} \tag{12}$$

According to Eq. (12), the black-box circuit of the quantum operation $\Omega_{Y,X}$ is demonstrated in Fig. 6.

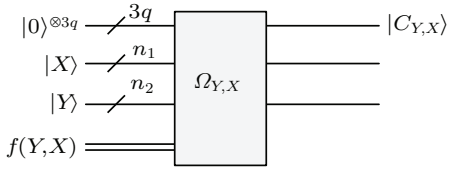


Fig. 6. The black-box quantum circuit of $\Omega_{Y,X}$.

3.4. Adder module

The function of adder module is to add n-qubit X and n-qubit Y by utilizing quantum Fourier transform (QFT).[29] The quantum circuit of adder module is shown in Fig. 7, which can be decomposed into three steps: QFT, rotation module and inverse QFT (IQFT). In order to realize the addition function, adder module only needs one auxiliary qubit, which improves the operation performance compared with the reversible parallel adder in Ref. [30].

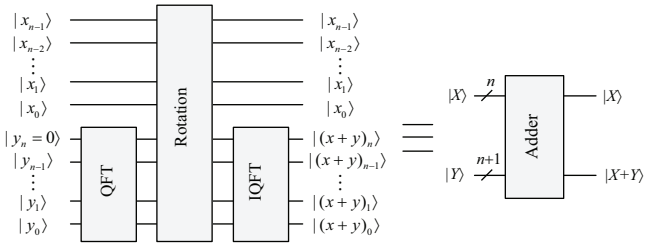


Fig. 7. The quantum circuit of adder module figure from Ref. [31].

3.5. Reversible subtractor module

The function of reversible subtractor (RS) module[32,33] is to subtract n-qubits X from n-qubits Y, and its quantum circuit is shown in Fig. 8, which contains two sub-modules: reversible half subtractor (RHS) and reversible full subtractor (RFS). The details of these two sub-modules are elaborated in Ref. [32].

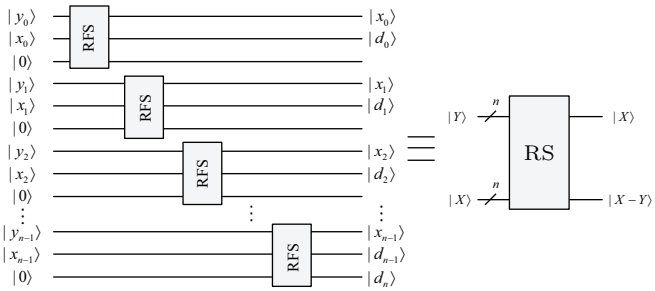


Fig. 8. The quantum circuit of RS module.

3.6. T-count multiplier module

The function of T-count multiplier (TM) module[34] is to multiply n-qubit X and n-qubit Y, and its corresponding quantum block diagram is shown in Fig. 9. The TM module consists Toffoli gate array and CtrAdd circuit, and the details are discussed in Ref. [34].

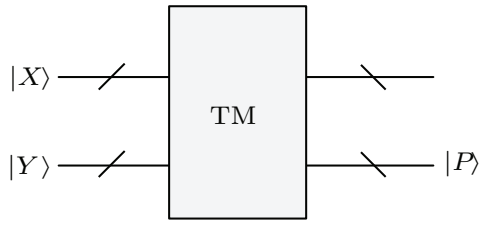


Fig. 9. The block diagram of TM module.

3.7. Divided by 2 module

The function of divided by 2 module[31] is to halve a nonnegative integer, which can be realized by utilizing two CNOT gates and $n-1$ quantum swap gates. For instance, the calculation procedure of employing divided by 2 module for $|x\rangle = |x_{n-1}x_{n-2}\ldots x_1x_0\rangle$ is discussed as below:

$$\begin{aligned}|x\rangle &= |x_{n-1}x_{n-2}\ldots x_1x_0\rangle \to |x_{n-1}x_{n-2}\ldots x_0x_1\rangle \\ &\to |x_{n-1}x_{n-2}\ldots x_0x_2x_1\rangle \\ &\to \cdots \to |x_{n-1}x_0x_{n-2}\ldots x_2x_1\rangle \\ &\to |x_0x_{n-1}x_{n-2}\ldots x_2x_1\rangle \approx |x/2\rangle\,, \end{aligned} \tag{13}$$

where $x_{n-1}x_{n-2}\ldots x_2x_1$ in final result $x_0x_{n-1}x_{n-2}\ldots x_2x_1$ is the calculated effective qubits.

Figure 10 shows the quantum circuit for realizing the above transformation.

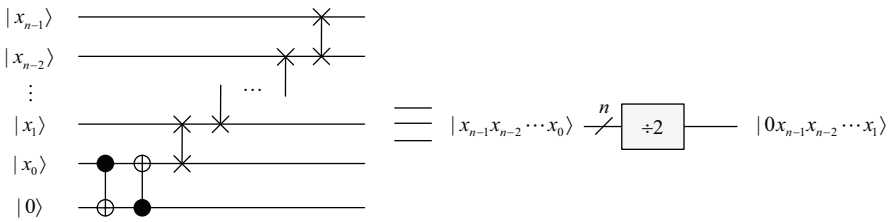


Fig. 10. The quantum circuit of divided by 2 module.

4. Quantum circuit realization of color image scaling

In this section, the concrete quantum color image scaling-up and scaling-down schemes based on the bilinear interpolation are discussed in detail. Assume that a $2^{n_1}\times 2^{n_2}$ color image $|I\rangle$ is represented by INCQI model, where the color depth of each RGB channel is q. Consequently, the color information and position information of $|I\rangle$ need to be represented by $3q$ qubits and (n_1+n_2) qubits, respectively. After designing the specific quantum circuits, the corresponding complexity is analyzed.

4.1. Quantum color image scaling-up scheme

Suppose a $2^{n_1}\times 2^{n_2}$ color image is enlarged to $2^{n_1+m_1}\times 2^{n_2+m_2}$ by utilizing bilinear interpolation, where n_1, n_2, m_1 and m_2 are all nonnegative integers. For the scaling ratios r_y and r_x in Y and X directions, the corresponding values are 2^{m_1} and 2^{m_2}, respectively. According to the principle of bilinear interpolation method, the color value $|C_{Y',X'}\rangle$ of the position (Y',X') in the interpolation image $|I'\rangle$ can be calculated from the color values of the four coordinates corresponding to the original image. Consequently, by utilizing Eqs. (8) and (9), the particular calculation formula of pixel value $|C_{Y',X'}\rangle$ is described by

$$\begin{aligned}|C_{Y',X'}\rangle &= (1-d_y)(1-d_x)|C_{Y,X}\rangle + (1-d_y)d_x|C_{Y,X+1}\rangle + d_y(1-d_x)|C_{Y+1,X}\rangle + d_yd_x|C_{Y+1,X+1}\rangle \\ &= \left[1-\left(\frac{Y'}{2^{m_1}}-Y\right)\right]\times\left[1-\left(\frac{X'}{2^{m_2}}-X\right)\right]\times|C_{Y,X}\rangle + \left[1-\left(\frac{Y'}{2^{m_1}}-Y\right)\right]\times\left(\frac{X'}{2^{m_2}}-X\right)\times|C_{Y,X+1}\rangle \\ &\quad + \left(\frac{Y'}{2^{m_1}}-Y\right)\times\left[1-\left(\frac{X'}{2^{m_2}}-X\right)\right]\times|C_{Y+1,X}\rangle + \left(\frac{Y'}{2^{m_1}}-Y\right)\times\left(\frac{X'}{2^{m_2}}-X\right)\times|C_{Y+1,X+1}\rangle \\ &= \left\{[2^{m_1}-(Y'-2^{m_1}\times Y)]\times[2^{m_2}-(X'-2^{m_2}\times X)]\times|C_{Y,X}\rangle + [2^{m_1}-(Y'-2^{m_1}\times Y)]\times(X'-2^{m_2}\times X)\times|C_{Y,X+1}\rangle\right. \\ &\quad + (Y'-2^{m_1}\times Y)\times[2^{m_2}-(X'-2^{m_2}\times X)]\times|C_{Y+1,X}\rangle \\ &\quad \left. + (Y'-2^{m-1}\times Y)\times(X'-2^{m_2}X\times)\times|C^{Y+1,X+1}\rangle\right\}\times(2^{m-1}\times 2^{m_2})^{-1}. \end{aligned} \tag{14}$$

From Eq. (14), the color value $|C_{Y',X'}\rangle$ of position (Y',X') is calculated by $|C_{Y,X}\rangle$, $|C_{Y,X+1}\rangle$, $|C_{Y+1,X}\rangle$ and $|C_{Y+1,X+1}\rangle$ in the original image $|I\rangle$. The detailed circuit of quantum color image scaling is shown in Fig. 11, where these gray-shaded areas are the core part of calculating the color weight of pixels. The following are the specific implementation procedures of color image scaling:

Step 1 Firstly, the four positions (Y,X), $(Y,X+1)$, $(Y+1,X)$ and $(Y+1,X+1)$ of the original image can be obtained through multiple CNOT and U_1 modules.

Step 2 Secondly, the four color values $|C_{Y,X}\rangle$, $|C_{Y,X+1}\rangle$, $|C_{Y+1,X}\rangle$ and $|C_{Y+1,X+1}\rangle$ in step 1 are calculated by quantum unitary operation $\Omega_{Y,X}$, $\Omega_{Y,X+1}$, $\Omega_{Y+1,X}$ and $\Omega_{Y+1,X+1}$. According to the characteristics of bilinear interpolation, the weight of each pixel can be obtained through multiple CNOT and RS modules.

Step 3 Finally, according to the calculation function in Eq. (14), $|C_{Y',X'}\rangle$ can be acquired by four TM modules, three adder modules and (m_1+m_2) divided by 2 modules.

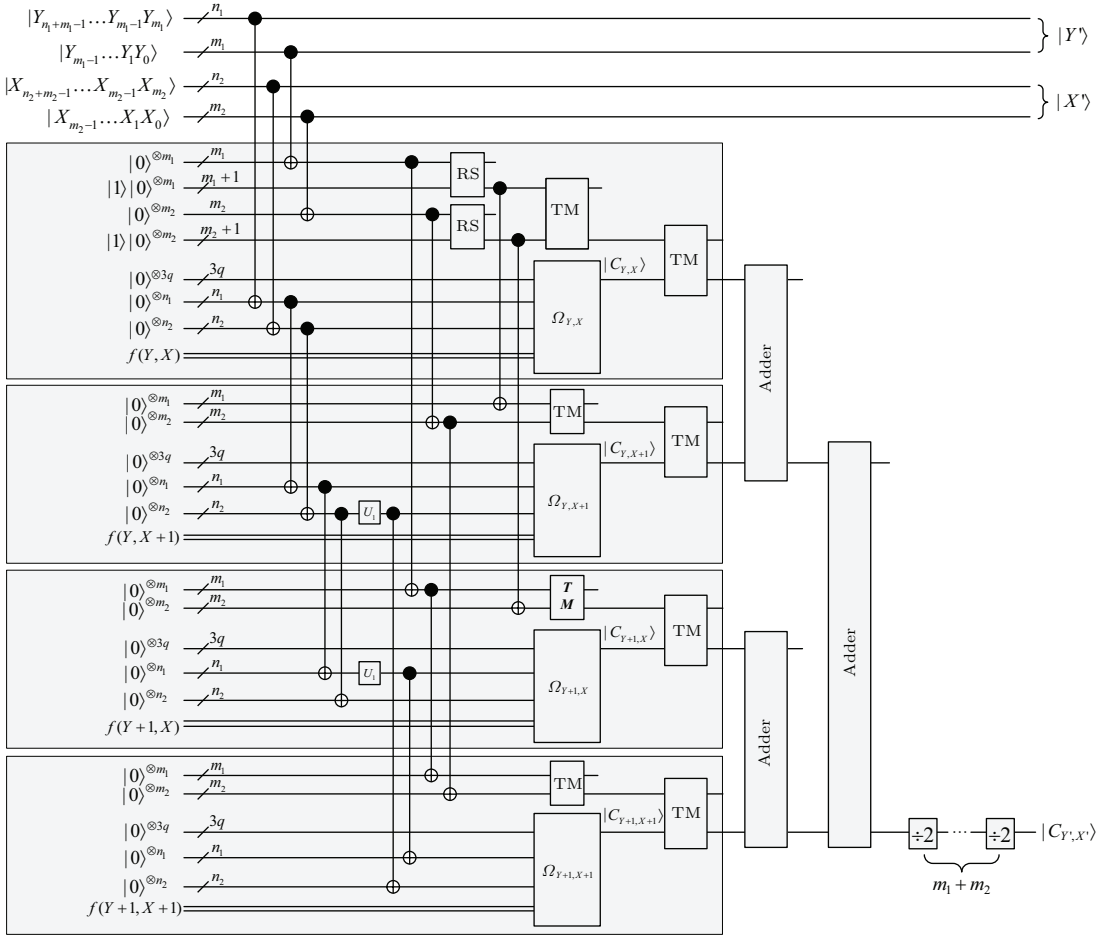


Fig. 11. The quantum color image scaling-up circuit based on Eq. (14).

4.2. Quantum color image scaling-down scheme

In this case, the scaling-down scheme of quantum color image based on INCQI model will be discussed. Assume a $2^{n_1}\times 2^{n_2}$ color image is reduced to $2^{n_1-m_1}\times 2^{n_2-m_2}$, where n_1, n_2, m_1 and m_2 are all nonnegative integers. At this point, the vertical and horizontal scaling ratios are $r_y=2^{-m_1}$ and $r_x=2^{-m_2}$, respectively. Due to the characteristics of image size, $n_1>m_1$, and $n_2>m_2$ are specified.

As with the scaling-up scheme, according to the bilinear interpolation method, the color value $|C_{Y',X'}\rangle$ of position (Y',X') in the interpolated image $|I'\rangle$ can be obtained from the color values of the four coordinates corresponding to the original image $|I\rangle$. By performing equivalent substitutions in Eqs. (8) and (9), the interpolated pixel value $|C_{Y',X'}\rangle$ can be described by

$$\begin{aligned}\left|C_{Y',X'}\right\rangle &= (1-d_y)(1-d_x)\left|C_{Y,X}\right\rangle+(1-d_y)d_x\left|C_{Y,X+1}\right\rangle\\ &\quad+d_y(1-d_x)\left|C_{Y+1,X}\right\rangle+d_yd_x\left|C_{Y+1,X+1}\right\rangle\\ &=\left[1-\left(\frac{Y'}{2^{-m_1}}-Y\right)\right]\times\left[1-\left(\frac{X'}{2^{-m_2}}-X\right)\right]\times\left|C_{Y,X}\right\rangle\\ &\quad+\left[1-\left(\frac{Y'}{2^{-m_1}}-Y\right)\right]\times\left(\frac{X'}{2^{-m_2}}-X\right)\times\left|C_{Y,X+1}\right\rangle\\ &\quad+\left(\frac{Y'}{2^{-m_1}}-Y\right)\times\left[1-\left(\frac{X'}{2^{-m_2}}-X\right)\right]\times\left|C_{Y+1,X}\right\rangle\\ &\quad+\left(\frac{Y'}{2^{-m_1}}-Y\right)\times\left(\frac{X'}{2^{-m_2}}-X\right)\times\left|C_{Y+1,X+1}\right\rangle. \quad (15)\end{aligned}$$

According to Eq. (8), $\frac{Y'}{2^{-m_1}}-Y$ and $\frac{X'}{2^{-m_2}}-X$ in the above equation can be further simplified as follows:

$$\begin{aligned}\frac{Y'}{2^{-m_1}}-Y &= Y'\times 2^{m_1}-\left\lfloor Y'\times\frac{2^{n_1}}{2^{n_1-m_1}}\right\rfloor\\ &= Y'\times 2^{m_1}-\left\lfloor Y'\times 2^{m_1}\right\rfloor=0,\\ \frac{X'}{2^{-m_2}}-X &= X'\times 2^{m_2}-\left\lfloor X'\times\frac{2^{n_2}}{2^{n_2-m_2}}\right\rfloor\end{aligned}$$

$$= X' \times 2^{m_2} - \left\lfloor X' \times 2^{m_2} \right\rfloor = 0. \tag{16}$$

Consequently, $\left|C_{Y',X'}\right\rangle$ in Eq. (15) can be equivalent replaced by Eq. (16), and the results are described as

$$\left|C_{Y',X'}\right\rangle = \left|C_{Y,X}\right\rangle. \tag{17}$$

As can be seen from Eq. (17), the pixel value $\left|C_{Y',X'}\right\rangle$ of position (Y',X') in the interpolated image $|I'\rangle$ ultimately determined by the pixel value $|C_{Y,X}\rangle$ of position (Y,X) in the original image $|I\rangle$. Therefore, the interpolation algorithm utilized in this case is not strictly the same as the traditional bilinear interpolation. Compared with the scaling-up scheme employed in this paper, the scaling-down scheme is relatively uncomplicated, and its corresponding circuit is shown in Fig. 12.

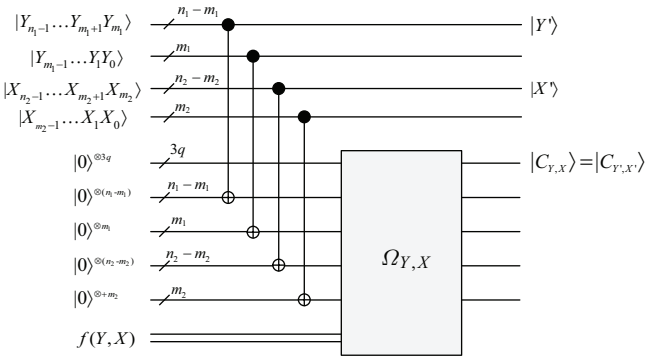


Fig. 12. The quantum color image scaling-down circuit based on Eq. (17).

4.3. Complexity analysis

In QImP, the complexity of quantum circuits depends on the number of elementary gates. The complexity of the quantum elementary gate is considered to be 1 including NOT gate, CNOT gate and any 2×2 unitary operator.[35] In addition, in order to complete the quantum computation, auxiliary qubits $|0\rangle$ or $|1\rangle$ are usually introduced in the design of quantum circuits. A series of quantum operations and quantum modules utilized in scaling circuits will be discussed below. And the complexity of the ultimate scaling circuits will be concluded at the end of this section.

4.3.1. Complexity of quantum modules

A series of quantum modules employed in the proposed scheme are described in Secttion 3, including multiple CNOT module, adding one module U_1, quantum operation $\Omega_{Y,X}$, adder module, reversible subtractor (RS) module, T-count multiplier (TM) module and divided by 2 module. Next, the complexity of these quantum modules mentioned above will be analyzed.

As shown in Fig. 4, in order to realize the replication of n-qubits $|Y\rangle$, n CNOT gates require to be utilized, so the complexity of multiple CNOT module is $O(n)$.

From Fig. 5, the quantum circuit of U_1 module can be decomposed into one CNOT gate, one Toffoli gate, one nCNOT gate and $(n-2)$ mCNOT gates $(m=3,4,\ldots,n)$. Reference [36] illustrated that an mCNOT gate $(m>3)$ can be equivalently converted to $2(m-1)$ Toffoli gates and one CNOT gate, and one Toffoli gate can be simulated by 6 CNOT gates. Consequently, a nCNOT gate is equivalent to $(12n-11)$ CNOT gates. For $(n-2)$ mCNOT gates, their conversion relationship with CNOT gate is as follows:

$$\begin{aligned}&(n-2)\,m-\text{CNOT gates}\\ =&\sum_{m=3}^{n} 2\,(m-1)\text{Toffoli gates}+(n-2)\,\text{CNOT gates}\\ =&\left(6n^2-5n-14\right)\text{CNOT gates}.\end{aligned} \tag{18}$$

In general, after the above analysis, the complexity of U_1 module can be expressed as $6n^2+7n-18$, i.e., $O(n^2)$.

For a $2^n\times 2^n$ quantum grayscale image with gray range 2^q, Ref. [9] points out that the complexity of the quantum operation $\Omega_{Y,X}$ is $O(q\cdot 2n)$. However, the $2^{n_1}\times 2^{n_2}$ quantum color image with color depth $3q$ is processed in this paper. Therefore, the corresponding complexity of $\Omega_{Y,X}$ is $O(3q\cdot(n_1+n_2))$.

From Fig. 8, the RS module is consisted of one RHS and $(n-1)$ RFS modules. Reference [33] points out that the quantum cost of RHS and RFS is 5 and 7, respectively. Therefore, the complexity of RS module is $O(n)$.

Reference [31] indicates that the complexity of adder module and divided by 2 module is $O(n^2)$ and $O(n)$, respectively. And according to Ref. [34], the complexity of TM module is $O(n^2)$.

4.3.2. Complexity of two quantum color image scaling circuits

Firstly, the complexity of the scheme of scaling $2^{n_1}\times 2^{n_2}$ color image to size $2^{n_1+m_1}\times 2^{n_2+m_2}$ is analyzed. The corresponding quantum circuit is shown in Fig. 11, which includes 16 multiple CNOT modules, 2 U_1 modules, 4 quantum operations $\Omega_{Y,X}$, 2 RS modules, 3 adder modules, m_1+m_2 divided by 2 modules and 8 TM modules. It is worth noting that the number of qubits required for color information and position information is diverse, but the number of qubits in the respective input part of TM module and adder module is required to be equal. Consequently, it is necessary to introduce auxiliary qubits to meet the above conditions. Before analyzing the overall complexity of the scaling-up scheme, it is assumed that $\alpha=\max\{3q,m_1,m_2\}$, which is the maximum number of qubits representing color and position information. Thus, based on the above assumption, the complexity of TM module and adder module in this case is $O(\alpha^2)$. Then, the complexity of the quantum circuit of the proposed scaling-up scheme is calculated as follows:

$$\begin{aligned}&O\big(4\,(n_1+n_2+m_1+m_2)+\left(n_1^2+n_2^2\right)\\ &+4\times 3q\,(n_1+n_2)+(m_1+m_2)+\alpha^2+(m_1+m_2)\,\alpha+\alpha^2\big)\\ \approx\;&O\left(n_1^2+n_2^2+\alpha^2+q\,(n_1+n_2)+(m_1+m_2)\,\alpha\right).\end{aligned} \tag{19}$$

For the proposed scaling-down scheme, it is relatively uncomplicated because only one quantum operation $\Omega_{Y,X}$ is employed in this method. From Fig. 12, four multiple CNOT modules and 1 quantum operation $\Omega_{Y,X}$ are utilized in this quantum circuit. Therefore, the analysis of the complexity of this circuit is particularly clear, that is,

$$\begin{aligned} &O\big((n_1-m_1)+m_1+(n_2-m_2)+m_2+3q(n_1+n_2)\big)\\ &\approx O(q(n_1+n_2)). \end{aligned} \tag{20}$$

4.3.3. Comparison of the complexity with other schemes

According to the above analysis of the complexity, it can be concluded that the complexity of our proposed scaling-up scheme is a quadratic function of the image size and color depth, and the complexity of scaling-down scheme is a linear function. As a comparison object, the complexity of enlarging $2^n \times 2^n$ to $2^{n+m} \times 2^{n+m}$ and reducing $2^{n+m} \times 2^{n+m}$ to $2^n \times 2^n$ schemes in Ref. [27] is the exponential functions $O\left(2^{n+3}\right)$ and $O(2^{n+m+3})$, respectively. Thus, it is obviously that the complexity of the proposed scheme is less than that in Ref. [27].

In addition, in order to prove the superiority of quantum computation in QImP, the complexity of the proposed scheme will also be compared with the classical image scaling scheme. In a classical computer, the digital images can only be processed pixel by pixel. Consequently, for a $2^{n_1} \times 2^{n_2}$ classical image is scaled to $2^{n_1+m_1} \times 2^{n_2+m_2}$ or $2^{n_1-m_1} \times 2^{n_2-m_2}$, its corresponding complexity is at least $O\left(2^{n_1+m_1+n_2+m_2}\right)$ or $O\left(2^{n_1-m_1+n_2-m_2}\right)$, which is the exponential function of the image size. Therefore, it is explicit that the complexity of classical scheme is much higher than the proposed scheme.

5. Simulation-based experiments and analysis

In this section, the proposed scheme will be compared with the scheme based on nearest-neighbor interpolation in Ref. [18]. Since the physical quantum computers are not yet universal and not yet accessible to us, the linear algebraic function in the MATLAB software package of the classical computer with Intel(R) Core(TM) i5-10210U CPU @1.60 GHz, SK Hynix 16 GB Ram equipped with the software MATLAB R2016a environment is utilized to carry out a series of simulation experimental evaluations, in which the complex vectors are used to represent quantum states and the unitary matrices denote unitary transformation. In addition, for recovering the classical images from quantum system, the quantum images need to be measured.

5.1. Experimental process of proposed scheme for INCQI

Figure 13 gives the concrete process of quantum color image scaling based on our scheme. Firstly, the INCQI model is utilized to convert a classical RGB color image into a quantum color image $|I\rangle$. Then, the quantum image is scaled based on the proposed scaling-up or scaling-down algorithm. Finally, the quantum measurement is performed on the quantum interpolated image $|I'\rangle$ to obtain the final classical interpolated image.

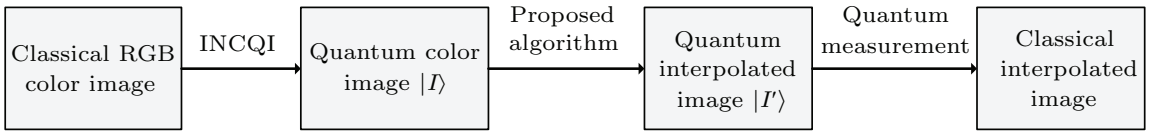
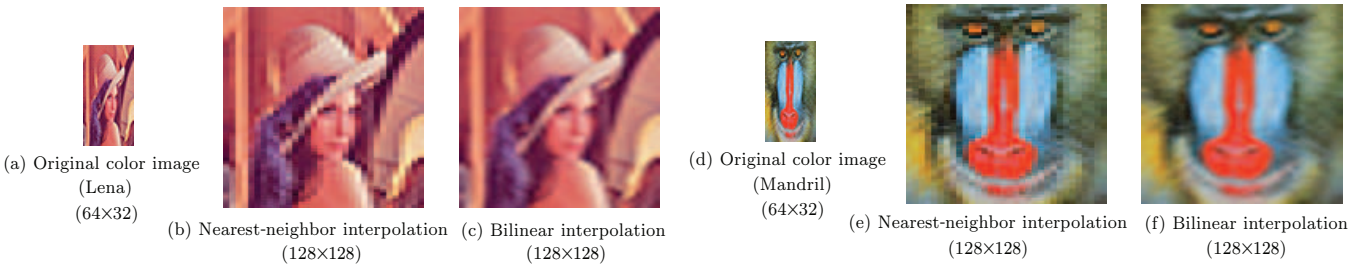


Fig. 13. The concrete experimental process of proposed scheme.

5.2. Comparison of simulation results

In order to reflect the advantages of the proposed scheme, the quantum color image scaling scheme based on nearest neighbor interpolation[18] is selected to compare with the proposed scheme. The simulation results based on different interpolation methods are shown in Figs. 14 and 15.

As shown in Figs. 14(a) and 14(d), two 64×32 original color images named Lena and Mandril, respectively. The corresponding scaling-up images based on the scheme of Ref. [18], which are given in Figs. 14(b) and 14(e). Figures 14(c) and 14(f) are the corresponding scaled-up images based on the proposed scheme. The above four interpolated images are all under the scaling-up ratios $r_y = 2$ and $r_x = 4$.

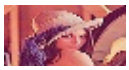


(a) Original color image (Lena) (64×32)
(b) Nearest-neighbor interpolation (128×128)
(c) Bilinear interpolation (128×128)
(d) Original color image (Mandril) (64×32)
(e) Nearest-neighbor interpolation (128×128)
(f) Bilinear interpolation (128×128)

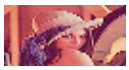
Fig. 14. Simulation results using different interpolation under $r_y = 2$ and $r_x = 4$.



(a) Original color image (Lena) (128×128)



(b) Nearest-neighbor interpolation (32×64)



(c) Bilinear interpolation (32×64)



(d) Original color image (Mandril) (128×128)



(e) Nearest-neighbor interpolation (32×64)



(f) Bilinear interpolation (32×64)

Fig. 15. Simulation results using different interpolation under $r_y = 1/4$ and $r_x = 1/2$.

For the proposed scaling-down scheme based on the extend bilinear interpolation, the corresponding simulation results under the scaling-down ratios $r_y = 1/4$ and $r_x = 1/2$ are shown in Fig. 15. Figures 15(a) and 15(d) are the 128×128 original color images named Lena and Mandril, respectively. Figures 15(b) and 15(e) show the interpolated images reduced by the nearest-neighbor interpolation mentioned in Ref. [18]. And the interpolated images using the proposed scheme are given in Figs. 15(c) and 15(f).

From our visual perspective, it is obvious that whether the original image Lena or Mandril in Fig. 14, the scaling effect of the proposed scheme is clearer than that of the nearest-neighbor interpolation scheme. The scaled images used by nearest-neighbor interpolation method show evidently jagged marks and mosaic phenomenon. And the images obtained by the proposed scheme are relatively smooth. However, the interpolated images in Fig. 15 based on the distinct interpolation are similar. That is because the extend bilinear interpolation employed in the proposed scaling-down scheme utilizes only one adjacent pixel, which is similar to the nearest-neighbor interpolation.

5.3. Quantum measurement of the interpolation image

An interpolation image based on INCQI model can be described as

$$\left|I'\right\rangle = \frac{1}{2^{\frac{n_1+n_2}{2}}} \sum_{Y'=0}^{2^{n_1}-1} \sum_{X'=0}^{2^{n_2}-1} \left|C\left(Y',X'\right)\right\rangle \otimes \rangle \left|Y'X'\right\rangle. \tag{21}$$

Apparently, an INCQI image is a quantum superposition state, which can be regarded as a composite quantum system consisting of (n_1+n_2+3q) qubits. Because a measurement in the quantum system will destroy the superposition, the quantum state cannot be actually observed. And according to the non-cloning theorem, it is not allowed to make copies of the state and measure each one. Consequently, in order to estimate the interpolated image, it is necessary to repeatedly construct the states of the interpolated image n $(n > 1)$ times and measure each state to summarize the measurement results. The probability measurement method is used to execute on the interpolated image, which transforms quantum information into classical information in the form of probability distributions, that is, a single qubit state $|\psi\rangle = \alpha|0\rangle + \beta|1\rangle$ is converted into a probability classical bit M (distinguish by drawing a double-line wire in quantum circuit), which is 0 with the probability $|\alpha|^2$ or 1 with the probability $|\beta|^2$ as shown in Fig. 16.

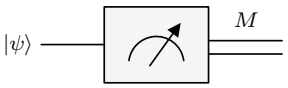


Fig. 16. The circuit symbol for quantum measurement.

Next, the influence of quantum measurement on the interpolated images will be discussed. The measurement results of the $2^{n_1+m_1} \times 2^{n_2+m_2}$ or $2^{n_1-m_1} \times 2^{n_2-m_2}$ interpolated image with color depth q for each channel are some collection of basis states $\{S_1, S_2, \ldots, S_{n_1+m_1+n_2+m_2+3q}\}$ and $\{S_1, S_2, \ldots, S_{n_1-m_1+n_2-m_2+3q}\}$, respectively.

These basis states adhere to the probability distribution after multiple quantum measurements. The interpolated images will continue to be measured util the probability of each basis state stabilized at a fixed value. According to the law of large numbers, there is a limit to these states used to estimate the color information of the interpolated image. The block diagram of the measurement operation on quantum computers is described in Fig. 17.

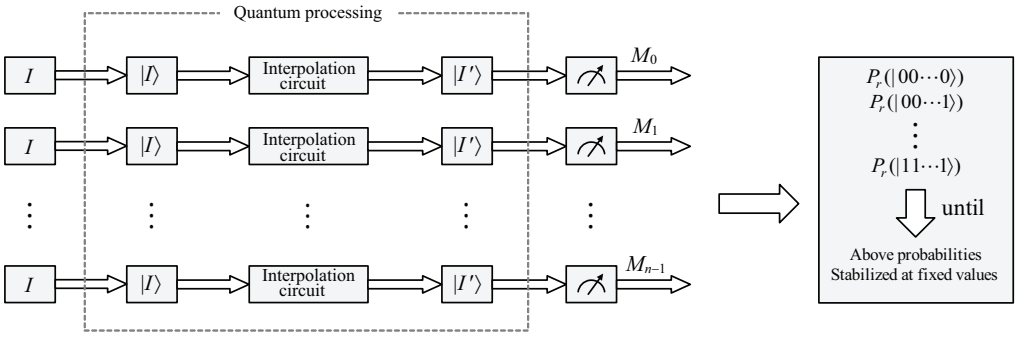


Fig. 17. The block diagram of measurement operation on quantum computers.

6. Conclusion

Quantum image processing aims to promote the transition from image applications by using the classical computing to the more advanced quantum computation. In this paper, a scheme of employing bilinear interpolation strategy to quantum color images represented by INCQI model is proposed for the first time. The proposed scheme mainly consists of the following two procedures to construct the interpolated images: (1) build the mapping relationship of pixels position, and (2) calculate the corresponding color information by utilizing the bilinear interpolation. According to the above two stages, the corresponding quantum circuit are designed to realize the scaling-up and scaling-down of quantum color images. In addition, the complexity of the two circuits is analyzed, and the simulation-based experiments are carried out to illustrate the advantages of the proposed scheme.

The main contributions of this paper are as follows: 1. A bilinear interpolation strategy for quantum color images based on INCQI representation is introduced for the first time. 2. The complexities of the two proposed scaling schemes are $O\left(n_1^2+n_2^2+\alpha^2+q\left(n_1+n_2\right)+\left(m_1+m_2\right)\alpha\right)$ and $O\left(q\left(n_1+n_2\right)\right)$, respectively, which are much lower than the exponential circuit complexity of Ref. [27]. Furthermore, the visual effect of the interpolated images based on the proposed scheme are obviously better than the scaling result in Ref. [27].

The future works mainly include: 1. The proposed scheme merely realizes the quantum color image scaling by integer multiple, so a quantum color image scaling scheme with arbitrary ratio can be designed. 2. The bicubic interpolation methods is mature in classical image processing because of its superior image scaling results. However, there is no relevant scheme in quantum image processing. Consequently, we can try to study the quantum image scaling based on the bicubic interpolation.

Acknowledgements

Project supported by the National Natural Science Foundation of China (Grant No. 6217070290) and Shanghai Science and Technology Project (Grant Nos. 21JC1402800 and 20040501500).

References

[1] Feynman R P 1982 *Int. J. Theor. Phys.* **21** 467
[2] Deutsch D 1985 *Proc. Royal Soc. London Ser. A* **400** 97
[3] Shor P W 1994 *Proceedings of* 35*th Annual Symposium on Foundations of Computer Science* pp. 124–134
[4] Grover L K 1996 *Proceedings of the* 28*th Annual ACM symposium on the Theory of Computing* pp. 212–219
[5] Venegas-Andraca S and Bose S 2003 *Proc. SPIE 5105, Quantum Information and Computation August* **4** 2003
[6] Latorre J I 2005 arXiv: quant-ph/0510031 [hep-ph]
[7] Venegas-Andraca S and Ball J 2010 *Quantum Inform. Proc.* **9** 1
[8] Le P Q, Dong F and Hirota K 2011 *Quantum Inform. Proc.* **10** 63
[9] Zhang Y, Lu K, Gao Y and Wang M 2013 *Quantum Inform. Proc.* **12** 2833
[10] Li H S, Zhu Q, Zhou R G, Song L and Yang X 2014 *Quantum Inform. Proc.* **13** 991
[11] Sang J, Wang S and Li Q 2017 *Quantum Inform. Proc.* **16** 42
[12] Le P Q, Iliyasu A M, Dong F Y and Hirota K 2010 *IAENG Int. J. Appl. Math.* **40** 113
[13] Hirota K, Dong F Y, Le P Q and Iliyasu A M 2011 *J. Adv. Comput. Intell. Intell. Informatics* **15** 698
[14] Zhang Y, Lu K, Xu K, Gao Y H and Wilson R 2015 *Quantum Inform. Proc.* **14** 1573
[15] Wang J, Jiang N and Wang L 2015 *Quantum Inform. Proc.* **14** 1589
[16] Jiang N and Luo W 2015 *Quantum Inform. Proc.* **14** 1559
[17] Jiang N, Wang J and Mu Y 2015 *Quantum Inform. Proc.* **14** 4001
[18] Zhou R G, Tan C Y, Fan P 2017 *Mod. Phys. Lett. B* **31** 1750184
[19] Chen G L and Song X H 2021 *Data Science* **1451** 453
[20] Jiang N, Wu W Y and Wang L 2014 *Quantum Inform. Proc.* **13** 1223
[21] Jiang N and Wang L 2014 *Quantum Inform. Proc.* **13** 1545
[22] Caraiman S and Manta V 2015 *Quantum Inform. Proc.* **14** 1693
[23] Zhou R G, Wu Q, Zhang M Q and Shen C Y 2013 *Int. J. Theor. Phys.* **52** 1802
[24] Zhou R G, Hu W and Fan P 2017 *Quantum Inform. Proc.* **16** 212
[25] Parker J, Kenyon R V and Troxel D E 1983 *IEEE Trans. Med. Imaging* **2** 31
[26] Zhou R G, Yang P L, Liu X A and Ian H 2018 *Int. J. Quant. Inf.* **16** 1850060
[27] Zhou R G, Hu W, Fan P and Ian H 2017 *Sci. Rep.* **7** 2511
[28] Le P Q, Iliyasu, A M, Dong F Y and Hirota K 2011 *Theor. Comput. Sci.* **412** 1406
[29] Ruiz-Perez L and Garcia-Escartin J C 2017 *Quantum Inform. Proc.* **16** 152
[30] Hafiz M Z, Begum Z, Islam M S and Rahman M M 2009 *Inf. Technol. J.* **8** 208
[31] Li P and Liu X 2018 *Int. J. Quantum Inform.* **16** 1850020
[32] Thapliyal H and Ranganathan N 2009 *Proceedings of the IEEE Computer Society Annual Symposium on VLSI, Tampa* pp. 229–234
[33] Thapliyal H and Ranganathan N 2011 *2011 11th IEEE Conference on Nanotechnology (IEEE-NANO), IEEE* pp. 1430–1435
[34] Muñoz-Coreas E and Thapliyal H 2019 *IEEE Trans. Comput.* **68** 729
[35] Barenco A, Bennett C H, Cleve R, Divincenzo D P, Margolus N, Shor P, Sleator T, Smolin J A and Weinfurter H 1995 *Phys. Rev. A* **52** 3457
[36] Nielsen M A and Chuang I L 2000 *Quantum Computation and Quantum Information* (Cambridge: Cambridge University Press)